

# Calorimetric Evidence for Two Distinct Molecular Packing Arrangements in Stable Glasses of Indomethacin

Kenneth L. Kearns, Stephen F. Swallen, and M. D. Ediger\*

Department of Chemistry, University of Wisconsin–Madison, Madison, Wisconsin 53706

Ye Sun and Lian Yu

School of Pharmacy, University of Wisconsin–Madison, Madison, Wisconsin 53705

Received: September 30, 2008; Revised Manuscript Received: December 6, 2008

Indomethacin glasses of varying stabilities were prepared by physical vapor deposition onto substrates at 265 K. Enthalpy relaxation and the mobility onset temperature were assessed with differential scanning calorimetry (DSC). Quasi-isothermal temperature-modulated DSC was used to measure the reversing heat capacity during annealing above the glass transition temperature  $T_g$ . At deposition rates near 8 Å/s, scanning DSC shows two enthalpy relaxation peaks and quasi-isothermal DSC shows a two-step change in the reversing heat capacity. We attribute these features to two distinct local packing structures in the vapor-deposited glass, and this interpretation is supported by the strong correlation between the two calorimetric signatures of the glass to liquid transformation. At lower deposition rates, a larger fraction of the sample is prepared in the more stable local packing. The transformation of the vapor-deposited glasses into the supercooled liquid above  $T_g$  is exceedingly slow, as much as 4500 times slower than the structural relaxation time of the liquid.

## Introduction

Unlike their crystalline counterparts, glasses have, in principle, a nearly infinite number of different structures. When a liquid is cooled, the molecules “get stuck” when their relaxation times exceed the time scale associated with cooling. The temperature where this arrest occurs is roughly the glass transition temperature  $T_g$ . Slower cooling delays the glass transition, and for many organic molecules, cooling 10 times more slowly lowers  $T_g$  by 3–5 K. Different cooling rates produce glasses with slightly different properties because they are formed from liquids with slightly different structures. Aging the nonequilibrium glass below  $T_g$  also alters properties but this requires a long time because molecular rearrangements in the glass are extremely slow.<sup>1,2</sup>

Physical vapor deposition can produce glasses that are significantly different than those produced by slowly cooling a liquid or aging an ordinary glass. Prior to 2007, the literature reported that vapor deposition prepared unstable materials with high enthalpy and low density.<sup>3–7</sup> This previous work utilized very cold substrates; under these conditions, molecules hit the substrate and have little opportunity to optimize packing before they are trapped. In contrast, we have shown that highly stable glasses can be formed by holding the substrate temperature  $T_{\text{substrate}}$  near  $0.85T_g$ .<sup>8–11</sup> Under these conditions, a liquidlike layer exists at the surface of the glass that allows incoming molecules to sample various local packing arrangements before they are trapped in the bulk glass by further deposition. As the deposition rate is lowered, molecules near the surface are given more time to sample different configurations and thus more stable materials are formed. For indomethacin (IMC) and tris(naphthylbenzene) (TNB), we have estimated that an ordinary glass would have to be aged for 1000 years or more to obtain glasses whose

enthalpy and density match those of the stable glasses prepared by vapor deposition.<sup>8</sup>

Systems that exhibit polyamorphism<sup>12</sup> can form glasses whose structures and properties vary significantly.<sup>13–18</sup> For crystals, distinct molecular packing motifs (polymorphs) are well documented for many systems. A particularly impressive case is ROY (5-methyl-2-[(2-nitrophenyl)amino]-3-thiophenecarbonitrile) where at least 10 polymorphs exist at ambient pressure and temperature.<sup>19</sup> Polyamorphism, by analogy, is the existence of more than one local packing arrangement in an amorphous system. Alternate packing arrangements, as detected by X-ray techniques, have been induced using pressure for a number of different organic,<sup>20,21</sup> inorganic,<sup>13,16</sup> and metallic systems<sup>17,18</sup> as well as elemental phosphorus.<sup>14,15</sup> Water has attracted considerable attention in this regard.<sup>16</sup> If water is vapor-deposited onto a cold substrate and then pressurized, an apparent first-order transition occurs near 6 kbar from low-density to high-density amorphous ice. Other systems including triphenyl phosphite<sup>20–24</sup> and  $Y_2O_3-Al_2O_3$ <sup>25,26</sup> show evidence for a first-order polyamorphic transition in the absence of pressure. A sharp exothermic peak during the transition from one equilibrium liquid phase to another has been presented as calorimetric evidence for polyamorphism in these two systems.<sup>23,24,26</sup> A theory of molecular liquids predicts that the well-studied glass formers *o*-terphenyl and toluene will undergo a polyamorphic phase transition below  $T_g$  if equilibrium could be attained at these low temperatures.<sup>27,28</sup> Despite numerous observations attributed to polyamorphism, the topic remains controversial. For instance, the apparent polyamorphism observed in triphenyl phosphite has been alternately interpreted as a poor crystal having only short-range order.<sup>29</sup> Experimental results from a broad range of techniques have been interpreted as supporting the concept of a poor crystal.<sup>30–33</sup>

Differential scanning calorimetry (DSC) experiments on stable vapor-deposited glasses of indomethacin show a surprising

\* To whom correspondence should be addressed. Email: ediger@chem.wisc.edu.

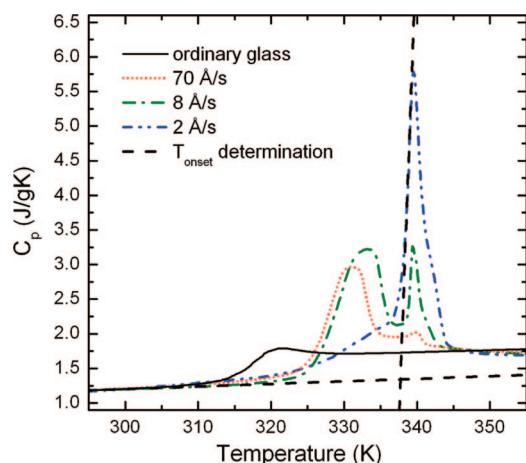


**Figure 1.** Total heat capacity  $C_p$  for vapor-deposited indomethacin glasses measured by conventional differential scanning calorimetry. For these samples, the deposition rates were 70 Å/s (dotted, red), 8 Å/s (dash-dot, green), and 2 Å/s (dash-dot-dot, blue);  $T_{\text{substrate}}$  was 265 K for each deposition. The  $C_p$  curve for an ordinary IMC glass (solid, black), prepared by cooling the liquid at approximately 40 K/min, is shown as well. Graphical determination of  $T_{\text{onset}}$  is shown (dash, black) for the 2 Å/s deposition; see details in text.

double-peaked structure,<sup>8</sup> which suggests the possibility of two different amorphous packings in this system. DSC measures the total heat capacity  $C_p$  during heating and typically an aged glass shows a single peak near  $T_g$ . This enthalpy relaxation peak (enthalpy “overshoot”) occurs whenever a low-enthalpy glass quickly transforms into the higher enthalpy supercooled liquid; the sudden flow of heat required to accomplish the transformation appears as a peak in  $C_p$ . Figure 1 shows an example of a double-peaked structure (curve labeled 8 Å/s) observed for a stable IMC glass. It is tempting to interpret these two peaks as two glass transitions resulting from two different types of molecular packing. Unfortunately, the DSC experiment is open to other interpretations. The key question is this: *When the sample has been heated through the first peak (but not the second), is the system a mixture of glass and liquid?* An affirmative answer is consistent with the idea that two distinct local packing arrangements are responsible for the two peaks; at an intermediate temperature, the less stable packing arrangement will have transformed into the liquid while the more stable packing arrangements remains glassy.

Here we have used quasi-isothermal temperature-modulated DSC (qi-TMDSC) to investigate the origin of the double-peaked structure in vapor-deposited IMC glasses. IMC was vapor-deposited onto substrates near  $0.85T_g$  at different rates. Conventional DSC and qi-TMDSC were employed on identical samples prepared in the same deposition. In a qi-TMDSC experiment, the sample temperature oscillates with a small amplitude about a fixed temperature. The qi-TMDSC technique measures the reversing portion of the heat capacity  $C_{p,\text{rev}}(t)$  as the sample isothermally transforms into the supercooled liquid somewhat above  $T_g$ . This observable discriminates between glass (no rearrangement during temperature cycling) and liquid (rapid rearrangement during temperature cycling) and is thus ideal to answer the question posed in the previous paragraph. In addition, the qi-TMDSC technique was used to quantify the isothermal stability of vapor-deposited IMC glasses at a number of annealing temperatures.

We find a two-step process in the qi-TMDSC experiments for all vapor-deposited IMC samples, over a deposition rate range from 70 to 0.8 Å/s. During annealing above  $T_g$ , first a

portion of the sample transforms into the liquid and then, after an intermediate incubation period, the rest of the sample transforms into the liquid. At lower deposition rates, a larger fraction of the sample transforms into the liquid in the second stage. These results are consistent with the idea that vapor deposition prepares a mixture of two different glasses of quite different stabilities. We also performed qi-TMDSC experiments on an ordinary IMC glass that had been aged for 37 days at room temperature. Unlike the vapor-deposited samples, the transformation of this glass to the supercooled liquid occurred in a single step. The kinetic stability of the vapor-deposited glasses increased as the deposition rate was lowered. For the lowest deposition rate, the transformation from the glass to the supercooled liquid was 4500 times slower than  $\tau_\alpha$ , the structural relaxation time of the supercooled liquid. The vapor-deposited samples exhibited greater kinetic stability than the ordinary glass that was aged for 37 days.

## Experimental Methods

**Materials.** Indomethacin (IMC) was purchased as the  $\gamma$  crystalline polymorph from Sigma (St. Louis, MO) and used without further purification. The chemical purity was greater than 99%. The melting temperature of the as-received material ( $T_m = 432.8$  K) agreed with literature data for the  $\gamma$  polymorph to within 1 K.<sup>34,35</sup>

**Vapor Deposition.** The vapor deposition process used here has been described previously.<sup>8,9</sup> Vapor deposition was performed in a vacuum chamber by heating the crystalline source material in a quartz crucible. IMC was deposited into aluminum DSC pans held 3 cm away from the source. The base pressure of the chamber was  $10^{-8}$  Torr. For a single deposition, three pans were used. Pans were attached to a copper cold stage and the temperature was controlled to within 1 K; for this study, all depositions were performed with  $T_{\text{substrate}} = 265$  K. Deposition rates were monitored with a quartz crystal microbalance and controlled by adjusting the temperature of the crucible. Depositions continued until 2–4 mg of sample had been deposited into each DSC pan resulting in films that were 30–60  $\mu\text{m}$  thick. The average deposition rate for a given sample pan is well-defined by the sample mass and the deposition time; this value is quoted in the text and figure captions. The deposition rate varied with time by less than 20% during any given deposition. Because the sample pan is close to the source, the deposition rate on one side of the pan could differ from that on the other side of the pan by as much as 30%.

**Conventional DSC Analysis.** The details of the DSC analysis have been described elsewhere.<sup>8,9</sup> One of the three pans from each deposition was analyzed using a TA Instruments Q2000 DSC. The sample mass was determined from the difference in pan mass before and after deposition. Data was acquired during three heating scans (10 K/min) for each pan. The first scan measured the total heat capacity  $C_p$  of the as-deposited glass. The sample was subsequently allowed to crystallize, and the second scan determined the  $C_p$  of the crystal through the melting point. The temperature of the melting point does not change before and after deposition; the deposition process does not result in the deposition of degradation products.<sup>8,9</sup> After the second scan, the sample was cooled at approximately 40 K/min into the glassy state. We refer to this glass as the “ordinary glass”. The third scan measured  $C_p$  for the ordinary glass. The change in  $C_p$  at  $T_g$  (third scan) and the heat of fusion (second scan) allow for checks on the sample mass. Throughout this paper, we refer to the onset temperature for the third scan (315

K) as  $T_g$  for IMC. This  $T_g$  value does not imply anything about the thermodynamic state or structure of any particular IMC glass.

**qi-TMDSC Analysis.** Quasi-isothermal temperature-modulated DSC (qi-TMDSC) measurements were performed using the TA Instruments Q2000 DSC. As with the conventional DSC analysis, calibration of the DSC instrument consisted of a baseline run along with indium and sapphire scans to calibrate the temperature and heat capacity, respectively. Prior to analysis, the samples were brought to room temperature (from storage at low temperature) and loaded into the calorimeter. Once the sample was loaded, the temperature was raised from room temperature to the isothermal annealing temperature  $T_{\text{anneal}}$  in about 200 s.  $T_{\text{anneal}}$  ranged from 317 to 325 K ( $T_g + 2$  to  $T_g + 10$ ). A periodic temperature modulation began as the temperature approached  $T_{\text{anneal}}$  with a period of 60 s and a peak-to-peak amplitude of 0.5 K. Time zero was defined as the point where  $T_{\text{anneal}}$  was initially reached. The amount of heat required to maintain the temperature modulation at the assigned value is proportional to the reversing heat capacity of the sample at that time and we denote this signal as  $C_{p,\text{rev}}(t)$ ; alternately, this signal can be regarded as the frequency-dependent specific heat, measured as a function of time at frequency  $f = 1/(60 \text{ s}) = 0.017 \text{ Hz}$ . The  $C_{p,\text{rev}}(t)$  data was considered reliable after one full period of oscillation had occurred after  $t = 0$ . After the qi-TMDSC experiment, conventional DSC experiments were performed to assess the amount of crystallization that occurred. Typically, 6% or less of the sample crystallized as determined by the change in  $\Delta C_p$  at  $T_g$ ; this has no impact on the interpretation of our results. In a few cases, a temperature modulation period of 120 s was used in the qi-TMDSC measurements. Within experimental error, identical results were obtained after the data was converted into  $\phi_{\text{glass}}(t)$ ; see eq 1 below.

According to the instrument manufacturer,  $C_{p,\text{rev}}$  measurements by qi-TMDSC on the TA Q2000 are accurate to 0.05 J/(g K). We confirmed this by measurements on a sapphire standard sample. As this uncertainty is not negligible compared to the differences of interest in these experiments, we handle the data as follows. Once the transformation from a glass to the liquid is completed, we assume that our sample has the heat capacity of the supercooled liquid and shift all the data so that it matches the measured  $C_{p,\text{rev}}$  for the supercooled liquid at  $T_{\text{anneal}}$ .

qi-TMDSC experiments were also performed on IMC samples that were prepared by cooling the liquid.  $C_{p,\text{rev}}$  values for the supercooled liquid (as shown in Figure 2) were obtained on ~10 mg samples of supercooled IMC prepared by melting IMC crystals in the DSC pan. Similar samples (5 mg) were used in aging experiments on ordinary IMC glasses (as shown in Figure 6).

The use of qi-TMDSC to isothermally monitor chemical and physical processes has been widely reported.<sup>36</sup> The chemical curing of an epoxy resin has been observed with qi-TMDSC;<sup>37</sup> as the system cures, the reversing heat capacity changes due to the change in structure with time. The isothermal crystallization of polymers<sup>38,39</sup> including polyethylene,<sup>40,41</sup> polyethylene terephthalate,<sup>42,43</sup> and PEEK<sup>44</sup> have also been studied using this technique. In all cases, accurate results are obtained if the sample does not evolve significantly in one modulation period. In our experiments, the modulation period is 60 s and the fastest transition from a vapor-deposited glass to the supercooled liquid requires more than 1000 s. The absence of any difference between experiments at modulation periods of 60 and 120 s supports this view that the modulation is fast enough to accurately measure  $C_{p,\text{rev}}$ .

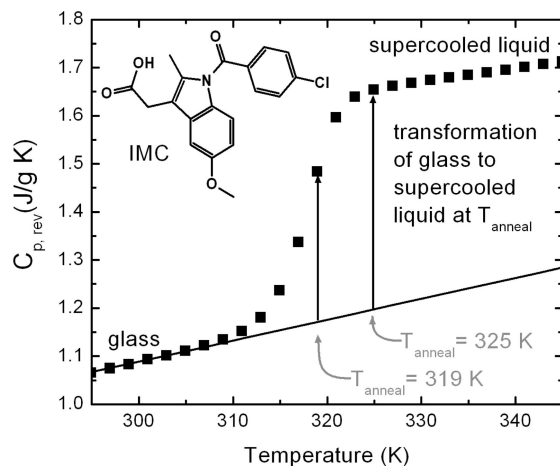


**Figure 2.** Reversing heat capacity  $C_{p,\text{rev}}$  for IMC supercooled liquid and glass measured with quasi-isothermal temperature-modulated DSC. For each measurement (squares), the period of the temperature oscillation was 60 s and the amplitude of the modulation was 0.5 K. The sample was prepared by cooling the liquid at 10 K/min. Data was collected isothermally for 300 s every 2 K beginning at 273 K.  $C_{p,\text{rev}}$  is larger at the highest temperatures because the temperature modulation drives configurational changes in the supercooled liquid. The solid line is a linear extrapolation of the glass  $C_p$ . The arrows schematically indicate the temperature jump experiments performed on stable vapor-deposited glasses (see below). Inset: Structure of IMC.

## Results

**Conventional DSC.** Figure 1 shows the total heat capacity  $C_p$  for indomethacin (IMC) glasses vapor-deposited at three different rates. For each of these depositions,  $T_{\text{substrate}}$  is held constant at 265 K ( $0.84T_g$ ) which was previously determined to be the optimal temperature for preparing stable glasses.<sup>9</sup> The black curve shows  $C_p$  for the ordinary glass; the glass transition temperature  $T_g$  is 315 K as defined by the onset of the transition. The shapes of the enthalpy overshoots (peaks in  $C_p$ ) change significantly as the deposition rate is lowered. In particular, double-peaked structures are observed at deposition rates of 8 and 70 Å/s. The position of the peak near 339 K is very nearly independent of deposition rate.

Figure 1 graphically defines  $T_{\text{onset}}$  as the intersection of a tangent drawn from the half-height of the  $C_p$  peak with the glass  $C_p$  line extrapolated to higher temperatures. Below  $T_{\text{onset}}$  the sample is too immobile to absorb the heat needed to become a liquid, but at  $T_{\text{onset}}$ , the molecules begin to move and an increase in heat capacity is observed; thus, a higher  $T_{\text{onset}}$  signifies greater kinetic stability. For vapor-deposited samples with two peaks,  $T_{\text{onset}}$  is clearly a flawed measure of kinetic stability. For example, should samples with two peaks be regarded as having two mobility onset temperatures, thus implying that they are composed of two different glasses? The quasi-isothermal experiments described next provide a way to answer this question.

**qi-TMDSC of Ordinary Glass and Supercooled Liquid.** Quasi-isothermal temperature-modulated DSC allows for the measurement of the reversing heat capacity  $C_{p,\text{rev}}$ . Reference qi-TMDSC measurements for indomethacin were first performed on the supercooled liquid and ordinary glass cooled from the melt. Figure 2 shows  $C_{p,\text{rev}}$  as a function of temperature for IMC. This sample was prepared by cooling the liquid into the glass at 10 K/min. For each measurement (squares), the period of the temperature oscillation was 60 s and the amplitude of the modulation was 0.5 K. Data was collected isothermally for 300 s every 2 K beginning at 273 K.



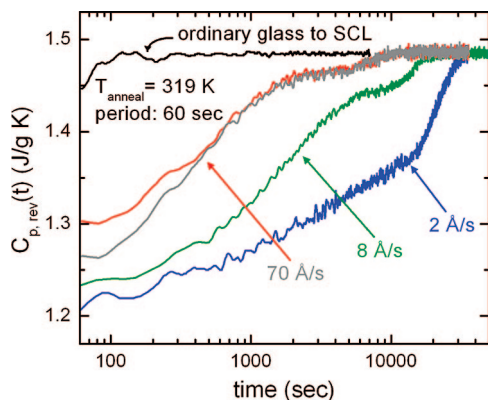


**Figure 3.** Reversing heat capacity  $C_{p,\text{rev}}$  as a function of time for vapor-deposited IMC glasses obtained from qi-TMDSC. Just prior to these measurements, the temperature was jumped up to 319 K. The steady increase of  $C_{p,\text{rev}}$  with time indicates the isothermal transformation of the glass into the supercooled liquid (SCL). Deposition rates for the samples are indicated. For reference,  $C_{p,\text{rev}}$  is also shown for an ordinary IMC glass prepared by cooling the liquid at 40 K/min.

The general features of Figure 2 are consistent with previous nonisothermal TMDSC work.<sup>45</sup> At low temperatures, IMC molecules are immobile on the time scale of the temperature modulation. The heat that flows into the sample to slightly increase the temperature goes completely into increasing the amplitude of vibrational motion in a system with fixed structure. At high temperatures, IMC molecules rearrange rapidly compared to the time scale of the temperature modulation. In this regime,  $C_{p,\text{rev}}$  is larger because increasing temperature requires both the energy to increase vibrational motion and the energy needed to change the structure of the liquid to the equilibrium structure at the new temperature. The step in  $C_{p,\text{rev}}$  is analogous to the step in  $C_p$  shown for the ordinary glass in Figure 1.

**qi-TMDSC of Vapor-Deposited Glasses.** The high kinetic stability exhibited by vapor-deposited IMC allows for the observation of the change in  $C_{p,\text{rev}}$  as a function of time during isothermal annealing. Conceptually, this experiment is illustrated by the vertical arrows in Figure 2. A temperature jump brings the stable glass sample to higher temperature. As the sample transforms into the supercooled liquid,  $C_{p,\text{rev}}$  will increase until it reaches the value for the supercooled liquid.

Figure 3 shows qi-TMDSC experiments on IMC glasses vapor-deposited at various rates. For a given deposition rate, the same deposition created multiple samples used for both scanning DSC analysis (Figure 1) and qi-TMDSC analysis (Figure 3). The annealing temperature  $T_{\text{anneal}}$  for each of the curves was 319 K. For all the vapor-deposited samples at short times,  $C_{p,\text{rev}}(t)$  is closer to the glass value of 1.17 J/(g K) than to the supercooled liquid value of 1.49 J/(g K); lower deposition rates systematically show lower initial values of  $C_{p,\text{rev}}$ . Additionally, the time required for the vapor-deposited samples to transform into the supercooled liquid value becomes much longer as the deposition rate is lowered; we have previously shown that lower deposition rates produce glasses lower on the energy landscape.<sup>8</sup> For comparison, we also show the qi-TMDSC experiment for an ordinary glass (black line). This sample finishes the transformation to the supercooled liquid in less than 100 s, at least 100 times faster than any of the vapor-deposited samples. (The value of 100 s for the ordinary glass transformation should be taken as an upper bound, given the difficulty in making accurate measurements in  $C_{p,\text{rev}}$  for rapid processes.)

The  $C_{p,\text{rev}}(t)$  curves in Figure 3 show a rich structure at intermediate times. Initially,  $C_{p,\text{rev}}(t)$  increases for all deposition

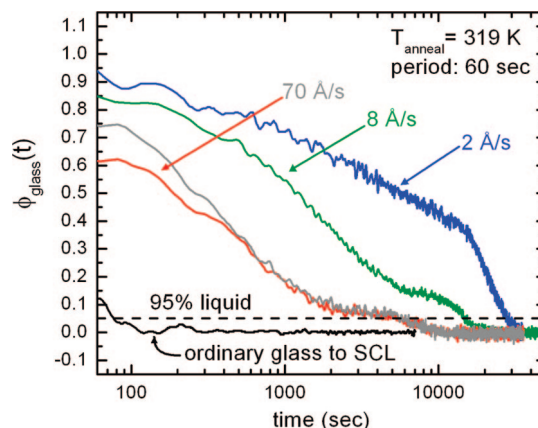


**Figure 4.** Fraction of the sample with glassy heat capacity  $\phi_{\text{glass}}$  as a function of time.  $\phi_{\text{glass}}(t)$  is calculated from the reversing heat capacity for vapor-deposited IMC glasses. The dashed horizontal line defines the  $\phi_{\text{glass}}$  value where 95% of the sample has transformed into the supercooled liquid.

rates. After the initial increase, a well-defined plateau in  $C_{p,\text{rev}}(t)$  is observed for the 70 and 8 Å/s data. The  $C_{p,\text{rev}}(t)$  data stops increasing for approximately 2500 s at both deposition rates; two samples are shown for depositions at 70 Å/s to emphasize the reproducibility of this feature (red and gray lines in Figure 3). After this plateau,  $C_{p,\text{rev}}(t)$  increases again until reaching the supercooled liquid value. For samples prepared at 2 Å/s,  $C_{p,\text{rev}}(t)$  does not show a clear plateau. After 15 000 s, however, the transformation to the supercooled liquid accelerates significantly as observed by the sharp increase in slope.

**Glass Fraction  $\phi_{\text{glass}}(t)$ .**  $C_{p,\text{rev}}(t)$  data can be converted to a function that expresses the fraction of the sample that responds to temperature modulation as a glass:

$$\phi_{\text{glass}}(t) = \frac{C_{p,\text{rev}}(\text{liquid}; T_{\text{anneal}}) - C_{p,\text{rev}}(t)}{C_{p,\text{rev}}(\text{liquid}; T_{\text{anneal}}) - C_{p,\text{rev}}(\text{glass}; T_{\text{anneal}})} \quad (1)$$

A  $\phi_{\text{glass}}(t)$  value of 1 indicates that the sample is 100% glass while a value of 0 indicates complete transformation to the supercooled liquid.  $C_{p,\text{rev}}(\text{glass}; T_{\text{anneal}})$  is determined by extrapolating the temperature dependence of the glass  $C_p$  to  $T_{\text{anneal}}$  while  $C_{p,\text{rev}}(\text{liquid}; T_{\text{anneal}})$  is determined by heating the ordinary glass and measuring for long times (data shown in Figure 2). Equation 1 is based upon one important assumption, i.e., that all glasses of a given molecule have the same  $C_{p,\text{rev}}$ . When carefully tested, this has been found to be true to better than 1%.<sup>46</sup> Even the crystal  $C_p$  is usually only a few percent different than the glass  $C_p$  for organic molecules.<sup>46</sup> Thus, we expect eq 1 to hold to an excellent approximation. One advantage of eq 1 (as opposed to the presentation in Figure 3) is that it allows a direct comparison between data acquired at different annealing temperatures.

Figure 4 shows the time-dependent glass fraction  $\phi_{\text{glass}}(t)$  at various deposition rates for IMC stable glasses annealed at 319 K. Of course, the general features of Figure 3 are apparent in Figure 4. The presentation in Figure 4 emphasizes that the 70 Å/s samples do not completely respond as a glass immediately after the temperature jump. The differences seen between the two 70 Å/s samples at initial times stems from the difficulty in obtaining absolute  $C_{p,\text{rev}}$  values to better than 0.05 J/(g K). This translates into a systematic uncertainty in absolute  $\phi_{\text{glass}}(t)$  values of about 15%. As the deposition rate is lowered to 2 Å/s, the initial  $\phi_{\text{glass}}$  value reaches unity within this uncertainty, indicating that the entire sample initially responds as a glass.

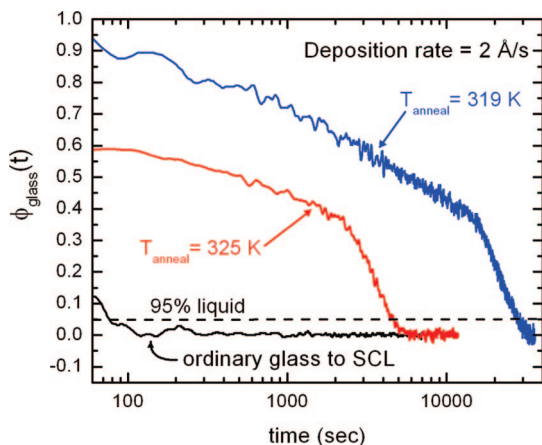


**Figure 5.** Effect of annealing temperature on  $\phi_{\text{glass}}(t)$  for IMC glasses vapor-deposited at 2 Å/s. The transformation into the supercooled liquid occurs more quickly at the higher temperature. Data for an ordinary glass prepared by cooling the liquid is shown for comparison ( $T_{\text{anneal}} = 319$  K).

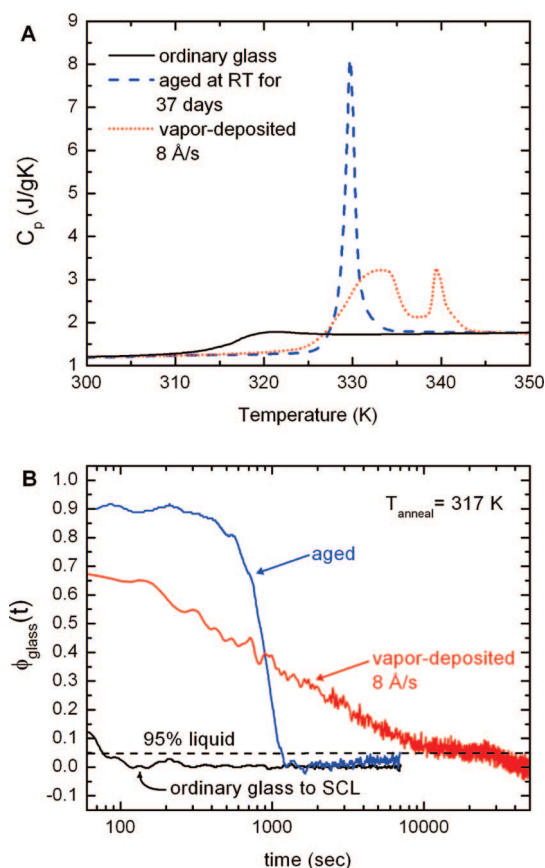


**Figure 6.** Comparison of IMC glasses prepared by vapor deposition and by aging an ordinary glass. The vapor-deposited sample (dotted, red) was prepared at 8 Å/s. The aged glass (dashed, blue) was prepared by cooling the liquid and aging at 295 K for 37 days. An unaged ordinary glass is shown for comparison. (A) Total heat capacity curves obtained from conventional DSC. (B)  $\phi_{\text{glass}}(t)$  data obtained from qi-TMDSC.  $T_{\text{anneal}}$  equals 317 K for the aged and vapor-deposited sample and 319 K for the ordinary glass.

Figure 5 shows the effect of annealing temperature on  $\phi_{\text{glass}}(t)$ . These samples were created during the same deposition, with a deposition rate of 2 Å/s. The higher  $T_{\text{anneal}}$  results in a faster overall transformation to the supercooled liquid as expected.  $\phi_{\text{glass}}(t)$  begins at a value of 0.6 for the higher annealing temperature indicating that a significant fraction of the sample

transformed into the supercooled liquid during the temperature step and the initial equilibration at 325 K. At the lower annealing temperature, the initial value of  $\phi_{\text{glass}}(t)$  is consistent with the sample being 100% glassy. The dashed horizontal line in Figures 4 and 5 indicates  $\phi_{\text{glass}} = 0.05$  and we use the time required to reach this line as a characteristic transformation time for a given sample. The transformation to  $\phi_{\text{glass}} = 0.05$  is more than 6 times faster at 325 K than at 319 K. A sharp change in the slope of  $\phi_{\text{glass}}(t)$  is observed for both samples at  $\phi_{\text{glass}} = 0.4$  (see below).

**Aged vs Vapor-Deposited Glasses.** One traditional way to produce kinetically stable glasses is to isothermally age a glass below  $T_g$ . Because glasses are not in equilibrium, they slowly relax toward the more thermodynamically stable supercooled liquid.

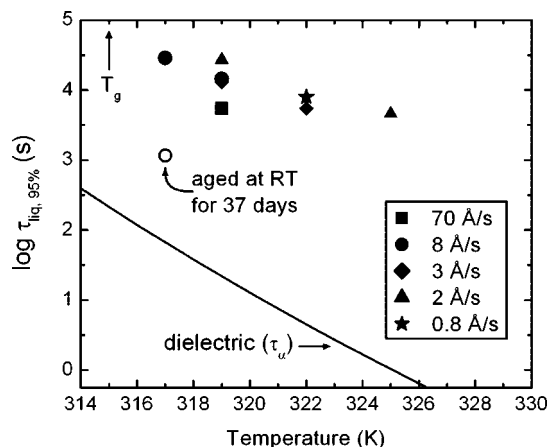
Figure 6 compares a vapor-deposited sample of IMC (8 Å/s) with an ordinary glass that was aged for 37 days at room temperature ( $\sim T_g - 20$  K); the aged ordinary glass is nearly in thermodynamic equilibrium (with respect to the supercooled liquid), as the fictive temperature value determined by DSC is nearly equal to the aging temperature. The conventional DSC measurements shown in Figure 6A indicate that the  $C_p$  peak from the aged sample is much sharper than the vapor-deposited sample. The vapor-deposited sample has a second peak in  $C_p$  about 10 K higher.

Figure 6B compares  $\phi_{\text{glass}}(t)$  data for the aged and vapor-deposited samples at  $T_{\text{anneal}} = 317$  K. Three major differences are observed. First, the initial value of  $\phi_{\text{glass}}$  is lower for the vapor-deposited IMC. Second, the time to transform 95% of the sample to the supercooled liquid is much longer for the vapor-deposited sample. The vapor-deposited IMC glass takes about 10 times longer to transform and slower deposition rates would further increase this ratio. Third, the shapes of  $\phi_{\text{glass}}(t)$  for the aged and vapor-deposited samples are quite different. An intermediate plateau is reached during the transformation of the vapor-deposited sample after about 10 000 s, which begins to evolve again after a total transition time of approximately 25 000 s. In contrast, the transformation of the aged glass to the supercooled liquid occurs in an autocatalytic, steplike manner.

**Dependence of Transformation Time on Deposition Rate and  $T_{\text{anneal}}$ .** To determine the influence of the deposition rate and annealing temperature on the transformation from the glass to the supercooled liquid, a series of qi-TMDSC experiments were performed. The deposition rate was varied from 70 Å/s down to 0.8 Å/s. The annealing temperature ranged from 317 K ( $T_g + 2$  K) to 325 K ( $T_g + 10$  K).

Figure 7 shows time required for 95% transformation ( $\tau_{95\%,\text{liq}}$ ) of the vapor-deposited IMC glasses (solid symbols) and the aged ordinary IMC glass (open circle). For reference, the solid line shows the VTF fit from dielectric relaxation data for the structural relaxation time  $\tau_\alpha$  for IMC obtained by Carpentier et al.<sup>47</sup> For all  $T_{\text{anneal}}$  and deposition rates, the time to transform 95% of the stable IMC glass into the supercooled liquid is much longer than  $\tau_\alpha$ . The transformation of the ordinary IMC glass aged at room temperature for 37 days is faster than the transformation for any of the vapor-deposited IMC samples.

The temperature dependence of the transformation times at a deposition rate of 2 Å/s appears to be weaker than the temperature dependence of  $\tau_\alpha$ . Similar results have been obtained using neutron reflectivity for stable glass films of tris(naphthylbenzene) (TNB).<sup>11</sup> In those experiments, TNB was vapor-deposited at a substrate temperature of 295 K ( $0.85T_g$ ) and at rates near 2 Å/s.



**Figure 7.** Time required to transform the glass into the supercooled liquid for vapor-deposited glasses and an aged ordinary glass, as a function of annealing temperature. The solid line is a VFT fit to dielectric relaxation measurements of the structural relaxation time  $\tau_\alpha$  for IMC by Carpentier et al.<sup>47</sup>

The different shapes of the time-dependent functions associated with  $\tau_\alpha$  and  $\tau_{95\%,liq}$  make their comparison somewhat arbitrary. We could also compare  $\tau_\alpha$  and the 1/e time for the isothermal transformation.  $\tau_{95\%,liq}$  was chosen instead to include the final stage of the isothermal transition from glass to supercooled liquid.

## Discussion

We have shown that quasi-isothermal temperature-modulated DSC experiments are useful for understanding the transformation of stable vapor-deposited IMC glasses into the supercooled liquid. qi-TMDSC can unambiguously determine the amount of time needed for transformation at a given temperature and thus quantify the kinetic stability of vapor-deposited IMC glasses. In this section, we briefly review the mechanism for the preparation of stable glasses. We then discuss the slow transformation of the stable glasses in the context of previous work on aged glasses. Finally, we argue that these experiments show that two distinct types of glass packing are present in vapor-deposited IMC glasses.

### Taking Advantage of Surface Mobility: Stable Glasses.

The mechanism by which vapor deposition can form stable glasses has been discussed elsewhere.<sup>8–10</sup> Here we briefly describe some aspects of the present results in this context. Many previous experiments have indicated that the dynamics at a glass surface are faster than dynamics in the bulk.<sup>48–54</sup> For IMC at  $T_g - 20$  K, we estimated this difference in dynamics to be approximately 7 orders of magnitude.<sup>8</sup> The thickness of the liquidlike region at the surface has been estimated to be a few nanometers at the substrate temperatures used here.<sup>10</sup> Enhanced surface dynamics allows stable glasses to be formed by vapor deposition if the temperature is near  $0.85T_g$ .<sup>9,10</sup> During deposition, molecules in the liquidlike layer sample configurations and find efficient packing arrangements. Further deposition buries these well-packed layers, and eventually a thick stable glass film can be prepared in this manner. Slower deposition allows more time for equilibration in the surface layer resulting in better-packed glasses with greater kinetic stability. Qualitatively, this explains the trends shown in Figure 4. Better-packed glasses have a harder time getting “unpacked” because larger activation barriers must be surmounted in this process.

**Kinetics of the Transformation from Stable Glass to Supercooled Liquid.** When an ordinary glass is heated above  $T_g$ , it quickly transforms into the supercooled liquid. The

dynamics under these conditions are dictated by the structural relaxation time  $\tau_\alpha$  of the supercooled liquid at the final temperature;  $\tau_\alpha$  is on the order of 10 s a few degrees above  $T_g$ . Aging an ordinary glass can significantly lengthen the transformation time. The transformation from the glass to supercooled liquid is often called structural recovery.

The results presented here can be compared to previous work on the structural recovery of aged glasses. Classic experiments on structural recovery were performed by Kovacs on poly(vinyl acetate) (PVAc).<sup>55</sup> PVAc was aged for long times at various temperatures below  $T_g$  ( $\sim 308$  K). The volume of the system was measured after the temperature was jumped from the aging temperature to an annealing temperature of 313 K. After aging for 2 months at 298 K, it took about 2500 s to reach the equilibrium volume at 313 K. Similar experiments with only 20 min of aging at 298 K took about 70 s to reach equilibrium at 313 K, and we use this latter value as our estimate of the equilibrium structural relaxation time  $\tau_\alpha$  at 313 K. Thus, the most highly aged glass that Kovacs prepared required about 35  $\tau_\alpha$  to completely transform to the liquid.

Stable vapor-deposited IMC glasses can be viewed as highly aged samples. The deposition rate is inversely related to aging time; the lower the deposition rate the longer the time that the molecules “age” in the mobile layer near the surface. We have previously estimated that an ordinary glass of TNB would need to be aged for at least 1000 years in order to reach the enthalpy and density of the most stable vapor-deposited TNB samples;<sup>8</sup> similar estimates are obtained for vapor-deposited IMC glasses. In light of this, the results shown in Figure 7 are not surprising. Transformation of the stable IMC glasses into the liquid requires between 250 and 4500  $\tau_\alpha$  at the annealing temperature, considerably longer than the PVAc glasses tested by Kovacs. In contrast, the ordinary glass of IMC that was aged for 37 days required about 20  $\tau_\alpha$  to transform into the liquid, in reasonable agreement with PVAc samples aged for similar periods of time.

Unlike samples prepared by aging ordinary glasses of IMC or PVAc, the transformation from the glass to the supercooled liquid takes place in a complex manner for vapor-deposited samples. For the Kovacs’ PVAc experiment, after the temperature was increased from the aging temperature below  $T_g$  to the annealing temperature above  $T_g$ , the volume response was autocatalytic. During a long induction time, little volume recovery was observed. Once the volume began to increase, the volume quickly reached that of the equilibrium supercooled liquid. Closely related behavior is observed for the aged IMC sample presented in Figure 6B. In contrast, none of the vapor-deposited glasses show this behavior. In all cases the sample begins to evolve into the supercooled liquid from the very beginning of the annealing period. In addition, each sample deposited at 8 Å/s or greater reaches an intermediate plateau where the sample stops transforming. In Figure 4 we observe that after the 8 Å/s sample has been annealed for approximately 15 000 s, 80% of the sample has transformed into the supercooled liquid; 2500 s (or 250  $\tau_\alpha$ ) later this fraction has not changed. Samples deposited at 70 Å/s show a plateau of similar length. After this intermediate induction time, the sample once again continues the transformation into the supercooled liquid.

**Distinct Molecular Packing Arrangements in Vapor-deposited IMC Glasses.** We take the view that this data establishes the existence of two distinct molecular packing arrangements in vapor-deposited IMC glasses. In this section, we present our argument and discuss the origin of these different packing arrangements.



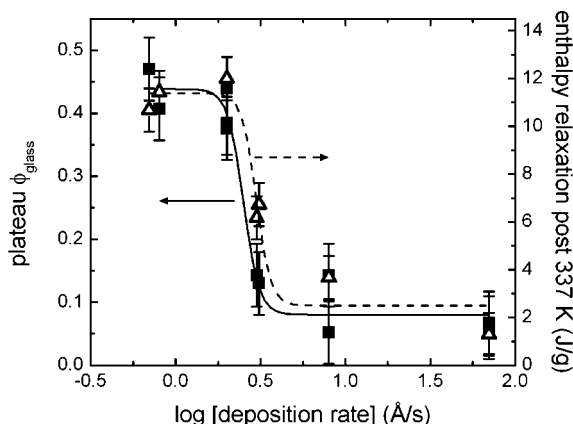


**Figure 8.** Changes in calorimetric observables with deposition rate for vapor-deposited IMC glasses. The fraction of the sample that remains glassy at the  $\phi_{\text{glass}}$  plateau is plotted on the left axis (filled squares). The area of the enthalpy relaxation peak after 337 K (open triangles) is plotted on the right axis. The similarity in these two observables as a function of deposition rate indicates that two different types of glasses are present in the vapor-deposited samples. The solid and dashed lines are sigmoidal fits and are intended to be guides to the eye. Error bars characterize variability among 2 to 6 samples.

The observation that  $\phi_{\text{glass}}(t)$  spends long periods of time with values intermediate between zero and unity establishes that the vapor-deposited samples at these intermediate times are a mixture of glass and liquid. The presence of intermediate induction times (plateau features) for samples deposited at 8 and 70 Å/s suggests that two glasses are present and that these glasses have different kinetic stabilities. It is likely that these two glasses have different fictive temperatures as well. Although these calorimetric experiments do not measure structure, we speculate that the significant difference in the kinetic stability indicated by the two-step decay in  $\phi_{\text{glass}}(t)$  must have a structural origin and we describe this as distinct local packing arrangements.

In the Introduction we posed a question about the two-peaked DSC curves shown in Figure 1: *When the sample has been heated through the first peak (but not the second), is the system a mixture of glass and liquid?* We can now answer definitively “yes” and we can show that the DSC curves should also be interpreted as indicating two different types of local packing. In Figure 8, we correlate the results of the conventional DSC experiment with those obtained by qi-TMDSC. The left axis shows the value of  $\phi_{\text{glass}}$  at which a plateau is observed in the isothermal experiment; at low deposition rates, we use the  $\phi_{\text{glass}}$  value at which a clear change in slope occurs as illustrated in Figure 5. The right axis shows the area of the high-temperature enthalpy relaxation peak in the conventional DSC experiment; it was calculated by integrating the area between the  $C_p$  curve for the stable glass and the supercooled liquid above 337 K. The two data sets show the same trend with deposition rate. Thus, it is clear that the high-temperature peak in the conventional DSC experiments correlates with the longer time decay process in the isothermal experiments. We attribute both of these features to the more stable of the two local packing arrangements. The correlation between the area of the enthalpy relaxation peak and amplitude of the longer time decay process can be seen directly in Figure 9.

We emphasize that the DSC and qi-TMDSC experiments do not measure the same observables. The qi-TMDSC is only sensitive to the reversing part of the heat flow and thus essentially probes the fraction of the sample that has the glass heat capacity at a given time. The conventional DSC experiment is sensitive to the total heat flow needed to increase the

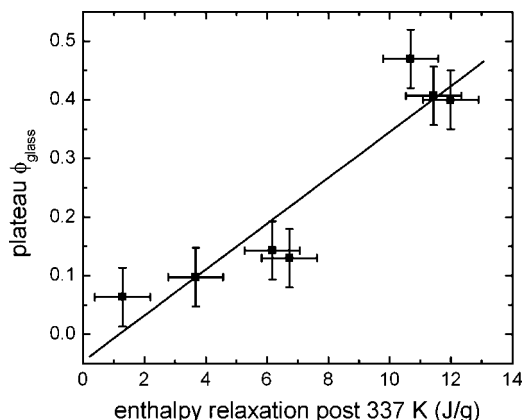


**Figure 9.** Correlation of conventional DSC and qi-TMDSC results for vapor-deposited IMC glasses. The fraction of the sample that remains glassy at the  $\phi_{\text{glass}}$  plateau (from qi-TMDSC) is plotted as a function of the area of the enthalpy relaxation peak post 337 K. The solid black line is the best linear fit. Error bars are standard deviations characterizing the range of values from 2 to 6 samples.

temperature; the peaks observed correspond to the heat required to raise the enthalpy of a low-enthalpy glass up to the liquid value.

In light of Figures 8 and 9, the conventional DSC curves can be qualitatively interpreted as indicating a sample with two glass transitions. The substantial peaks in  $C_p$  indicate that both glasses have low enthalpies compared to the liquid. The considerable difference in temperature between the two peaks (6–8 K) indicates a significant difference in kinetic stability for the two glasses. We speculate that high deposition rates primarily create a glass similar in structure to the one created by aging an ordinary glass. At lower deposition rates, an increasingly large fraction of sample is formed in a much more stable packing arrangement.

Finally, we would like to comment on the possible connection between these results and polyamorphism. For a number of different systems, a first-order transition from one amorphous phase to another has been reported.<sup>13–18,20–26</sup> In some cases, sharp exothermic signatures are observed from calorimetry and attributed to the transition of one equilibrium liquid to the other.<sup>24,26</sup> The two different types of local packing that we discuss here could be associated with two different amorphous states. It may be that the more stable of the two packing arrangements is thermodynamically stable only below some transition temperature between the substrate temperature and  $T_g$ . The more stable packing arrangement would thus be practically inaccessible to IMC samples prepared by cooling the liquid. On the other hand, because of rapid molecular motion near the glass surface, this state could be accessed during the deposition process. We regard this scenario as an intriguing possibility but, in the absence of evidence of a first-order phase transition in IMC, it is only speculation.

## Conclusions

Physical vapor deposition was used to prepare glasses of indomethacin using a substrate temperature of 265 K and deposition rates ranging from 70 to 0.8 Å/s. Conventional DSC was used to measure the total heat capacity of these glasses during heating. A complex double-peaked curve was observed at deposition rates near 8 Å/s. Quasi-isothermal temperature-modulated DSC was used to measure the reversing heat capacity at 0.017 Hz, providing an accurate assessment of the fraction of the sample with a glassy response as a function of annealing

time. The transformation of the vapor-deposited glasses to the supercooled liquid was extremely slow, requiring up to 4500  $\tau_\alpha$  at  $T_g + 10$  K. This slow transformation takes place in a two-step process; after some fraction of the glass has transformed into the supercooled liquid, an intermediate induction time is observed.

We interpret the two peaks in the total  $C_p$  curves and the two-step transformation in  $C_{p,rev}$  as evidence for two distinct molecular packing arrangements in the vapor-deposited glasses. As the sample is annealed above  $T_g$ , the less stable glass packing transforms into the supercooled liquid first. The more stable glass packing transforms into the supercooled liquid only at much longer times or, in the case of conventional DSC, at higher temperature. Samples deposited at lower rates contain more of the higher stability packing arrangement.

The appearance of two distinct stable glasses in a single-component organic system is surprising and may be evidence for polyamorphism in IMC. It is possible that vapor-deposition onto substrates near  $0.85T_g$ , due to configurational sampling below the conventional  $T_g$ , uniquely provides access to the glass associated with a new liquid state. Further experiments on indomethacin and other glass formers are required to test this hypothesis.

**Acknowledgment.** This work was supported by the National Science Foundation (CHE-0724062).

## References and Notes

- (1) McKenna, G. B. In *Comprehensive Polymer Science*; Booth, C., Price, C., Eds.; Pergamon: Oxford, UK, 1989; p 311.
- (2) Thureau, C. T.; Ediger, M. D. *J. Chem. Phys.* **2002**, *116*, 9089.
- (3) Hikawa, H.; Oguni, M.; Suga, H. *J. Non-Cryst. Solids* **1988**, *101*, 90.
- (4) Ishii, K.; Nakayama, H.; Okamura, T.; Yamamoto, M.; Hosokawa, T. *J. Phys. Chem. B* **2003**, *107*, 876.
- (5) Oguni, M.; Hikawa, H.; Suga, H. *Thermochim. Acta* **1990**, *158*, 143.
- (6) Takeda, K.; Yamamuro, O.; Oguni, M.; Suga, H. *Thermochim. Acta* **1995**, *253*, 201.
- (7) Takeda, K.; Yamamuro, O.; Suga, H. *J. Phys. Chem.* **1995**, *99*, 1602.
- (8) Kearns, K. L.; Swallen, S. F.; Ediger, M. D.; Wu, T.; Sun, Y.; Yu, L. *J. Phys. Chem. B* **2008**, *112*, 4934.
- (9) Kearns, K. L.; Swallen, S. F.; Ediger, M. D.; Wu, T.; Yu, L. *J. Chem. Phys.* **2007**, *127*, 154702.
- (10) Swallen, S. F.; Kearns, K. L.; Mapes, M. K.; Kim, Y. S.; McMahon, R. J.; Ediger, M. D.; Wu, T.; Yu, L.; Satija, S. *Science* **2007**, *315*, 353.
- (11) Swallen, S. F.; Kearns, K. L.; Satija, S.; Traynor, K.; McMahon, R. J.; Ediger, M. D. *J. Chem. Phys.* **2008**, *128*, 214514.
- (12) Wolf, G. H.; Wang, S.; Herbst, C. A.; Durben, D. J.; Oliver, W. J.; Kang, Z. C.; Halvorsen, C. In *High Pressure Research: Applications to Earth and Planetary Sciences*; Syono, Y., Manghnani, M. H., Eds.; American Geophysical Union: Washington, DC, 1992; p 503.
- (13) Deb, S. K.; Wilding, M.; Somayazulu, M.; McMillan, P. F. *Nature* **2001**, *414*, 528.
- (14) Katayama, Y.; Inamura, Y.; Mizutani, T.; Yamakata, M.; Utsumi, W.; Shimomura, O. *Science* **2004**, *306*, 848.
- (15) Katayama, Y.; Mizutani, T.; Utsumi, W.; Shimomura, O.; Yamakata, M.; Funakoshi, K. *Nature* **2000**, *403*, 170.
- (16) Mishima, O.; Calvert, L. D.; Whalley, E. *Nature* **1985**, *314*, 76.
- (17) Sen, S.; Gaudio, S.; Aitken, B. G.; Leshner, C. E. *Phys. Rev. Lett.* **2006**, *97*, 025504.
- (18) Sheng, H. W.; Liu, H. Z.; Cheng, Y. Q.; Wen, J.; Lee, P. L.; Luo, W. K.; Shastri, S. D.; Ma, E. *Nat. Mater.* **2007**, *6*, 192.
- (19) Chen, S. A.; Xi, H. M.; Yu, L. *J. Am. Chem. Soc.* **2005**, *127*, 17439.
- (20) Cohen, I.; Ha, A.; Zhao, X. L.; Lee, M.; Fischer, T.; Strouse, M. J.; Kivelson, D. *J. Phys. Chem. B* **1996**, *100*, 8518.
- (21) Hedoux, A.; Guinet, Y.; Derollez, P.; Hernandez, O.; Paccou, L.; Descamps, M. *J. Non-Cryst. Solids* **2006**, *352*, 4994.
- (22) Kurita, R.; Tanaka, H. *Science* **2004**, *306*, 845.
- (23) Tanaka, H. *Phys. Rev. E* **2003**, *68*, 011505.
- (24) Tanaka, H.; Kurita, R.; Mataka, H. *Phys. Rev. Lett.* **2004**, *92*, 025701.
- (25) Aasland, S.; McMillan, P. F. *Nature* **1994**, *369*, 633. Greaves, G. N.; Wilding, M. C.; Fearn, S.; Langstaff, D.; Kargl, F.; Cox, S.; Vu Van, Q.; Majerus, O.; Benmore, C. J.; Weber, R.; Martin, C. M.; Hennet, L. *Science* **2008**, *322*, 566.
- (26) Wilding, M. C.; McMillan, P. F. *J. Non-Cryst. Solids* **2001**, *293*, 357.
- (27) Matyushov, D. V.; Angell, C. A. *J. Chem. Phys.* **2005**, *123*, 034506.
- (28) Matyushov, D. V.; Angell, C. A. *J. Chem. Phys.* **2007**, *126*, 094501.
- (29) Kivelson, D.; Tarjus, G. *J. Non-Cryst. Solids* **2002**, *307*, 630.
- (30) Dvinskikh, S.; Benini, G.; Senker, J.; Vogel, M.; Wiedersich, J.; Kudlik, A.; Rossler, E. *J. Phys. Chem. B* **1999**, *103*, 1727.
- (31) Hedoux, A.; Guinet, Y.; Descamps, M.; Benabou, A. *J. Phys. Chem. B* **2000**, *104*, 11774.
- (32) Hedoux, A.; Hernandez, O.; Lefebvre, J.; Guinet, Y.; Descamps, M. *Phys. Rev. B* **1999**, *60*, 9390.
- (33) Wiedersich, J.; Kudlik, A.; Gottwald, J.; Benini, G.; Roggatz, I.; Rossler, E. *J. Phys. Chem. B* **1997**, *101*, 5800.
- (34) Crowley, K. J.; Zografi, G. *J. Pharm. Sci.* **2002**, *91*, 492.
- (35) Wu, T.; Yu, L. *J. Phys. Chem. B* **2006**, *110*, 15694.
- (36) Simon, S. L. *Thermochim. Acta* **2001**, *374*, 55.
- (37) VanAssche, G.; VanHemelryck, A.; Rahier, H.; VanMele, B. *Thermochim. Acta* **1996**, *286*, 209.
- (38) Pyda, M.; Di Lorenzo, M. L.; Pak, J.; Kamasa, P.; Buzin, A.; Grebowicz, J.; Wunderlich, B. *J. Polym. Sci. Polym. Phys.* **2001**, *39*, 1565.
- (39) Wunderlich, B. *Prog. Polym. Sci.* **2003**, *28*, 383.
- (40) Toda, A.; Oda, T.; Hikosaka, M.; Saruyama, Y. *Thermochim. Acta* **1997**, *293*, 47.
- (41) Toda, A.; Oda, T.; Hikosaka, M.; Saruyama, Y. *Polymer* **1997**, *38*, 231.
- (42) Okazaki, I.; Wunderlich, B. *Macromolecules* **1997**, *30*, 1758.
- (43) Toda, A.; Tomita, C.; Hikosaka, M.; Saruyama, Y. *Polymer* **1997**, *38*, 2849.
- (44) Wurm, A.; Merzlyakov, M.; Schick, C. *Colloid Polym. Sci.* **1998**, *276*, 289.
- (45) Shamblin, S. L.; Tang, X. L.; Chang, L. Q.; Hancock, B. C.; Pikal, M. J. *J. Phys. Chem. B* **1999**, *103*, 4113.
- (46) Chang, S. S.; Bestul, A. B. *J. Chem. Phys.* **1972**, *56*, 503.
- (47) Carpentier, L.; Decressain, R.; Desprez, S.; Descamps, M. *J. Phys. Chem. B* **2006**, *110*, 457.
- (48) Bell, R. C.; Wang, H. F.; Iedema, M. J.; Cowin, J. P. *J. Am. Chem. Soc.* **2003**, *125*, 5176.
- (49) Ellison, C. J.; Torkelson, J. M. *Nat. Mater.* **2003**, *2*, 695.
- (50) Forrest, J. A.; Dalnoki-Veress, K.; Stevens, J. R.; Dutcher, J. R. *Phys. Rev. Lett.* **1996**, *77*, 2002.
- (51) Kawana, S.; Jones, R. A. L. *Phys. Rev. E* **2001**, *6302*, 021501.
- (52) Keddie, J. L.; Jones, R. A. L.; Cory, R. A. *Faraday Discuss.* **1994**, *98*, 219.
- (53) Fakhraai, Z.; Forrest, J. A. *Science* **2008**, *319*, 600.
- (54) Sasaki, T.; Shimizu, A.; Mourey, T. H.; Thureau, C. T.; Ediger, M. D. *J. Chem. Phys.* **2003**, *119*, 8730.
- (55) Kovacs, A. J. *Fortsch. Hochpolym-Forsch.* **1963**, *3*, 394.

JP808665T